Virology Journal

RESEARCH

Open Access

Selection and identification of an ssDNA aptamer against influenza B virus hemagglutinin protein

Xing Lu[1,3†], Weifeng Li[1†], Ping Li[1], Yongqiang Li[1], Yanni Gou[3], Tao Wang[3], Zhifeng Liu[2*] and Yuting Wu[1,3,4*]

Abstract

Background The influenza virus causes infectious respiratory disease with high morbidity and mortality worldwide. Influenza B typically goes unnoticed owing to its mild clinical symptoms and limitations. However, its increasing prevalence in recent years poses a significant health burden. Consequently, current diagnostic methods for the detection of influenza B virus are inadequate, highlighting the urgent need to develop accurate and sensitive techniques for early disease diagnosis. Aptamers, single-stranded deoxyribonucleic acid (ssDNA), or ribonucleic acid molecules primarily rely on their secondary structures, such as stem-loops and hairpins, to bind efficiently and specifically to the target through base complementary pairing, electrostatic interaction, hydrogen bonding, and van der Waals forces. Aptamers are superior to antibodies in their ability to bind targets. The objective of this study was to identify and develop aptamers against the hemagglutinin (HA) protein of influenza B virus.

Methods An enriched DNA library with strong binding to the influenza B virus HA protein was obtained using magnetic bead systematic evolution of ligands by exponential enrichment technology after nine rounds of selection. Five candidate aptamers were identified by high-throughput sequencing. The aptamers were characterized using surface plasmon resonance and enzyme-linked immunosorbent assay techniques, and the aptamer exhibiting the highest affinity and specificity for the target protein was selected.

Results We screened and characterized five ssDNA aptamer sequences that bind to influenza B virus HA. Among these, aptamer sequence A573 exhibited the highest sensitivity and binding affinity for the target protein.

Conclusions The novel aptamer sequences selected in this study have the potential to be used as biorecognition molecules for the development of aptamer sensors to detect influenza B virus.

Keywords Aptamer, Influenza B virus, Hemagglutinin, Bead-SELEX, ELISA

†Xing Lu and Weifeng Li contributed equally to this work.

*Correspondence:
Zhifeng Liu
zhifengliu7797@163.com
Yuting Wu
yutingwu66@126.com
[1] Department of Respiratory and Critical Care Medicine, General Hospital of Southern Theater Command of PLA, No.111, Liuhua Road, Yuexiu District, Guangzhou 510010, Guangdong, China
[2] Department of Critical Care Medicine, General Hospital of Southern Theater Command of PLA, Yuexiu District, No.111, Liuhua Road, Guangzhou 510010, Guangdong, China
[3] Graduate School, Guangzhou University of Chinese Medicine, Guangzhou, China
[4] The First School of Clinical Medicine, Southern Medical University, Guangzhou, China

Background

Influenza is a highly contagious acute respiratory disease. Since the emergence of SARS-CoV-2, the spread of seasonal influenza virus has decreased significantly in 2020–2021; however, it increased in 2021–2022 [1]. Influenza B virus is a single-stranded negative-sense RNA virus with hemagglutinin (HA), which is a vital glycoprotein antigen located on its surface. HA plays a pivotal role in stimulating the body to generate neutralizing antibodies and is particularly prone to antigenic variation [2–4]. Consequently, HA is a crucial target for the development of antiviral medications and vaccines. Influenza B viruses primarily infect humans [5]. Although outbreaks caused by the influenza B virus are typically smaller and less severe than those caused by influenza A [6], they remain persistent seasonal epidemics and are frequently associated with complications that can be equally or even more detrimental than those caused by influenza A. In recent years, influenza B viruses have been reported to cause severe illness and mortality, contributing to over 20% of all influenza cases annually [7]. In individuals aged ≥ 50 years, the clinical morbidity and mortality rate of influenza B can reach up to 2.5% [8]. Diagnosing influenza B can often be a complex task because its symptoms tend to overlap with those of other respiratory infections, including those caused by SARS-CoV-2, H1N1, and others. Therefore, it is crucial to prioritize the rapid administration of influenza B testing and diagnosis immediately after symptoms appear to ensure that patients receive timely and effective treatment.

Currently, three main methods are used to diagnose influenza globally: traditional viral isolation and culture, immunodetection, and molecular biology-based diagnosis. Traditional methods rely on viral isolation and serological testing, which are complex and time consuming, making them unsuitable for widespread clinical use. Molecular biology diagnostic techniques such as PCR and fluorescence detection systems are cumbersome and costly. Immunodetection methods use specific antibodies against influenza viral antigens, which although highly sensitive, are prone to degradation; they are also expensive to obtain. DNA aptamers are increasingly recognized as potential molecules for the development of diagnostic methods for targets such as influenza because of their unique binding characteristics [9, 10].

Aptamers are a class of single-stranded nucleic acid sequences composed of DNA or RNA and are also known as nucleic acid aptamers. These molecules are typically identified through an in vitro selection process known as SELEX [11]. The SELEX method was designed to isolate oligonucleotide fragments from a vast library of nucleic acid molecules and select those with a high degree of specificity and affinity for specific targets. Aptamers are often described as "chemical antibodies" because of their ability to bind to targets with a high level of affinity and specificity, sometimes surpassing that of natural antibodies [12]. Compared to conventional antibodies, aptamers offer several benefits, including smaller size, reduced production costs, minimal or no immunogenicity, potential for various chemical modifications, a broad spectrum of targetable molecules, and the ability to achieve consistent batch-to-batch reproducibility [13]. Given their ease of synthesis and modification and their versatility in targeting, nucleotide aptamers hold significant promise for applications in viral detection and antiviral treatments [14]. A study has proposed a method for the detection of SARS-CoV-2 that employs an aptamer-based approach, which involves the binding of the spike protein through functionalized biomimetic nanochannels [15]. Previous research has focused on identifying aptamers for subtypes of influenza virus A [16]; however, there remains a scarcity of such aptamers specifically for influenza B viruses.

This study aimed to select the viral surface glycoprotein HA as a target molecule and use bead-based SELEX technology to screen for specific aptamers against the HA protein. The aptamers selected in this study have the potential to become new diagnostic or therapeutic tools for the detection and treatment of influenza B.

Methods

The objective of this study was to identify and develop aptamers against the influenza B virus HA protein. The target protein was fixed onto magnetic beads and combined with a random library, followed by PCR amplification. Single-stranded nucleic acids were separated using denaturing urea polyacrylamide gel electrophoresis to create a secondary library. Positive selection with HA protein of the influenza A virus, H1N1, ensured that the selected DNA aptamers were specific.

DNA library and primers

A library of ssDNA consisting of 76-mers, which included random 36-nucleotide sequences, was supplied by Sangon Biotechnology (Shanghai, China). Primers were obtained from GenScript Biotech (Nanjing, China). The sequences are listed in Table 1.

(i) 36N denotes 36 random oligonucleotides; (ii) within the primer designation, S1 signifies forward primer, A2 signifies reverse primer, and S1-FAM signifies the forward primer that is fluorescently labeled; (iii) A2-polyA refers to the reverse primer with a polyA tail attached, while polyA denotes a polyA tail composed of 19 adenosine residues; within the primer sequence, "Spacer 18" represents the 18-atom hexaethylene glycol spacer.

Table 1 Initial SELEX DNA library and primers

Name	Sequence (5′~3′)
LibP1	TTCAGCACTCCACGCATA GC-(36N)-CCTATGCGTGCTACC GTGAA
S1	TTCAGCACTCCACGCATAGC
A2	TTCACGGTAGCACGCATAGG
S1-FAM	FAM-TTCAGCACTCCACGCATAGC
A2-polyA	AAAAAAAAAAAAAAAAA A-Spacer18-TTCACGGTAGCA CGCATAGG

In vitro selection of aptamers

A protein screening kit (Cat no.: SEP-201904) was purchased from Anhui Aptamy Biotechnology Co. (Anhui, China)., and the following experiments were performed.

Library dissolution

Initially, a concentration of 1 optical density (OD) of libP1 library was diluted to 10 μm with Dulbecco's phosphate-buffered saline (DPBS) buffer (NaCl 137 mM, KCl 2.7 mM, Na_2HPO_4 8 mM, KH_2PO_4 1.5 mM, $CaCl_2$ 1 mM, $MgCl_2$ 0.5 mM, pH 7.4), and subsequently stored at −20 °C.

Carboxylated magnetic beads linked to positive and negative selection proteins

During each selection cycle, a typical 1-(3-dimethylaminopropyl)-3-ethylcarbodiimide hydrochloride (EDC)/N-hydroxysuccinimide (NHS) protocol was used to conjugate the HA protein onto the surface of the magnetic beads. Carboxylated magnetic beads (50 μL) were utilized and subjected to four washes, each with 200 μL of ultrapure water. The supernatant was then removed using a magnet. Subsequently, 50 μL of a 0.4 M EDC aqueous solution, previously thawed at 4 °C, and 50 μL of a 0.1 M NHS aqueous solution were rapidly combined and introduced to the washed beads. The resulting mixture was incubated on a shaker at ambient temperature for 20 min. If aggregation of magnetic beads was observed throughout the incubation period, the beads were gently agitated intermittently. Following incubation, a magnet was employed to separate the supernatant, and the magnetic beads were rinsed with 200 μL of DPBS. Subsequently, 10 μL of bovine serum albumin (BSA) solution at a concentration of 5 mg/mL was extracted and combined with 90 μL of sodium acetate (NaAC) buffer, which was adjusted to a pH of 4.0. The resulting mixture was subsequently introduced into cleaned magnetic microspheres. The mixture was agitated on a shaker at room temperature and was incubated for 50 min. In the case of aggregation of the magnetic beads during this period, intermittent agitation was applied. The supernatant was removed using a magnet. Next, 100 μL of a 1 M ethanolamine solution adjusted to pH 8.5, was introduced to the bead carriers within the experimental setup. Samples were incubated for 10 min at ambient temperature on a shaking platform with intermittent agitation to prevent aggregation. Subsequently, the supernatant was carefully aspirated using a magnetic stand and the beads were washed four times, each involving 200 μL of DPBS. The beads, designated MB-BSA, were conjugated to positively charged sieve proteins. The conjugation process with these positively charged sieve proteins was analogous. Upon activation of the magnetic beads, 10 μL of HA protein at a concentration of 2.31 mg/mL was combined with either 40 μL or 90 μL of NaAC at pH 5.5. The beads were then cleaned, incubated, and washed four times. The resulting product was designated as MB-HA for further use.

Positive/negative selection of library

Initially, library denaturation was performed, beginning with the library that was diluted to a concentration of 10 μM. The mixture was then subjected to high-speed centrifugation at 12,000 rpm for 10 min. Subsequently, 140 μL of DPBS was added for resuspension. One hundred microliters was distributed into each PCR tube and inserted into a PCR machine for denaturation. The following steps were applied: (1) temperature maintained at 95 °C for 10 min and (2) prompt immersion in an ice-water bath for 5 min to reach room temperature. This was labeled pool 0. Library positive selection involved the addition of 50 μL of MB-BSA to pool 0. The solution was mixed gently by pipetting. The mixture was then incubated in a shaker for 60 min at room temperature. Subsequently, the magnetic beads were positioned using a magnet, and the supernatant was aspirated with a pipette and labeled as pool-. The magnetic beads were rinsed with 200 μL of DPBS four times. The magnetic beads were oriented using a magnet and 200 μL of DPBS was added to the beads and heated in a water bath for 10 min. Subsequently, the beads were magnetically separated, and the supernatant was collected and designated as r-elution. For library positive selection, 50 μL of MB-HA was added to the pool following positive selection. The positive selection procedure was identical to that used for negative selection. The final supernatant was recorded as the R-Elution + Fluorescence Quantitative PCR Assay; a Roche 8-liner PCR tube array was used. The QPCR mix (28 μL) was dispensed into each well, ensuring that the mixture was subjected to a low-temperature melting phase ranging from 4 to 20 °C.

Subsequently, the supernatant acquired from rinsing of both the reverse and positive selection was introduced, encompassing r-elution, R-Elution+, and a 2 μL aliquot from a designated tube. One tube filled with blank QPCR mix was reserved, and 2 μL of screening buffer was added as a negative control. The fluorescence quantitative PCR protocol was as follows: initial denaturation at 95 °C for 2 min; followed by 30 cycles of denaturation at 95 °C for 1 min, annealing at 60 °C for 1 min, and extension at 72 °C for 1 min; and a final extension at 72 °C for 5 min.

Single-stranded DNA production

PCR products were concentrated in n-butanol. The concentrated PCR products were mixed with an equal volume of 2×TBE urea loading buffer, heat-denatured in a boiling water bath for 10 min to separate the DNA strands, and immediately loaded onto an electrophoresis gel after a brief spin. All samples were subjected to electrophoresis on urea-denaturing polyacrylamide gels at 300 V, until the bromophenol blue dye front reached the bottom of the gel. This procedure enabled FAM-labeled ssDNA to hybridize with complementary ssDNA that had been extended with a PolyA tail. The urea-denaturing polyacrylamide gel solution consisted of 5 mL of PAGE gel mix, 40 μL of 10% ammonium persulfate (APS), and 9 μL of *N*,*N*,*N*′,*N*′-tetramethylethylenediamine (TEMED). The gel was excised to recover the FAM-labeled strand. Initially, the gel was extracted and placed on a plastic film. Using a sterile blade, the desired band was directly excised and transferred into a 0.5 mL Eppendorf tube containing crushed gel. Subsequently, the tube was inserted into a 1.5 mL Eppendorf tube. This procedure was replicated by transferring 0.5 mL of the fragmented gel into a 1.5 mL microfuge tube, spinning at 12,000 rpm for 2 min, adding 1 mL of DPBS to a 1.5 mL microfuge tube, heating for 10 min, spinning again at 12,000 rpm for 1 min, aspirating the supernatant into a 15 mL centrifuge tube, and then repeating the steps of DPBS addition and heating. The supernatant was transferred into a 15 mL centrifuge tube and mixed with a specific volume of n-butanol. After thorough mixing, the mixture was centrifuged at 7500×*g* for 5 min. The resulting solution exhibited stratification, which allowed the upper and lower layers to be carefully aspirated and recovered, respectively. The lower layer was transferred to a microdialysis container, sealed with a nucleic acid dialysis membrane, and secured with a fixation ring to prevent liquid leakage. The microdialysis device was subsequently placed into 50 mL centrifuge tubes filled with 40 mL of screening buffer and incubated at 4 °C overnight to facilitate dialysis and extraction of the secondary library, which consisted of ssDNA. The concentrations of secondary libraries were measured using a NanoDrop 2000 spectrophotometer.

Nine rounds of screening were conducted using the magnetic bead-SELEX technique (Fig. 1) with the secondary library from the preceding round serving as the starting library for each subsequent operation. To enhance the affinity of the screened aptamers throughout the process, the incubation period for each step was reduced progressively. Starting from the second round of screening, the H1N1 HA protein was used for reverse screening. Table 2 details the incubation parameters and concentrations of the target proteins and ssDNAs.

High-throughput sequencings

High-throughput sequencing was conducted by examining qPCR results from each screening cycle. An upward trend and a greater retention rate for positive screenings were observed compared with those for negative screenings. After analyzing the enriched library using high-throughput sequencing, specific sequences were selected for synthesis by Universal Biosynthesis and subsequent affinity testing.

Surface plasmon resonance (SPR) detection

The SPR chip was cleaned three times using 50 mM aqueous NaOH solution. Subsequently, the chip was activated using an activation-mixed solution. Following activation, the HA protein was diluted in a NaAC aqueous solution adjusted to pH 5.5 (10 mM), resulting in a final concentration of 10 μg/mL. The diluted HA protein was injected into the target protein channel. Upon injection, the target protein channel was sealed with ethanolamine hydrochloride (pH 8.5). The coupling amount of HA protein was determined to be 15,296 RU. The chip was reactivated with the activation mixture and the control channel was subsequently sealed with ethanolamine hydrochloride (pH 8.5). Kinetic parameters were established using an SPR instrument (GE Healthcare, Biacore T200). The aptamer samples were diluted with buffer to create a gradient, which was then sequentially passed through the control and target protein channels. Each sample was regenerated using 1 M NaCl.

Analysis of aptamer properties with direct ELISA

The specificity and affinity (dissociation constant (Kd)) of the potential aptamer were determined using ELISA. The proteins were diluted to the specified concentrations, encapsulated in 96-well plates, and incubated overnight at 4 °C. Following this, the plates were thoroughly rinsed with washing buffer; a closure solution was dispensed into each well and incubated at 37 °C for 2 h. Thereafter, the liquid from the wells was removed and a diluted aptamer solution was introduced into each well. The

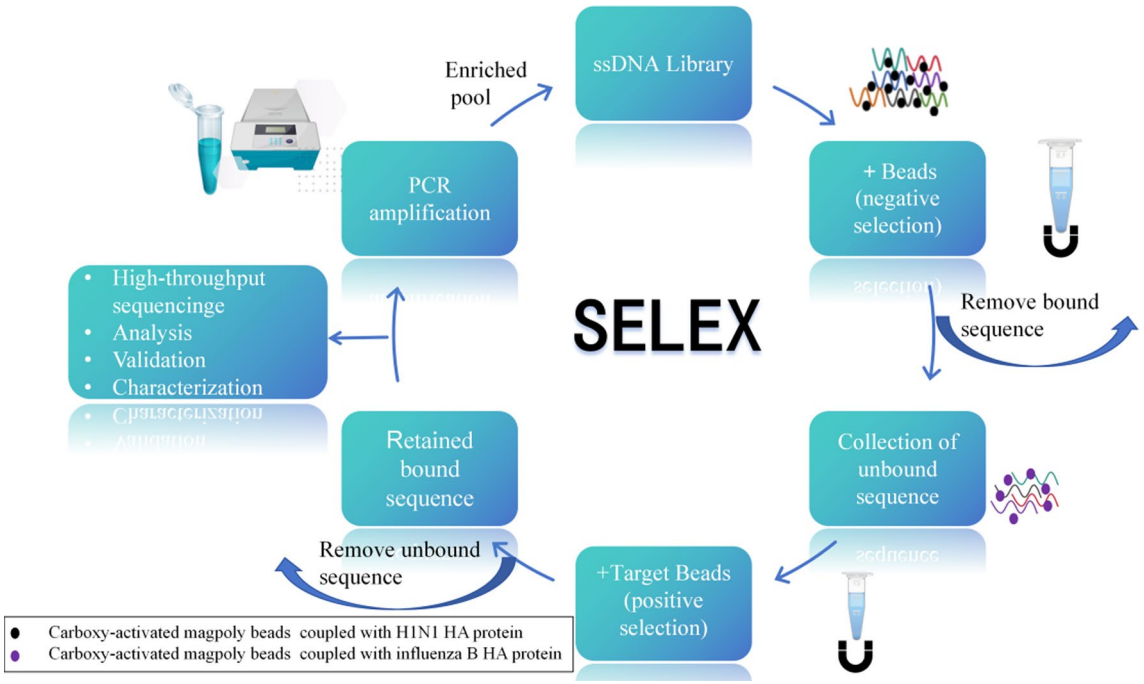

Fig. 1 Schematic representation of the beads-SELEX process for selecting aptamers against influenza B viral HA protein. The initial selection of high-affinity aptamers involves utilizing an ssDNA library. The aptamer library is first exposed to magnetic beads conjugated with the H1N1 HA protein. Sequences that bind to the beads are then subjected to a washing process, during which non-specific sequences are removed, and only the specifically bound sequences are retrieved and purified. Subsequently, the library is amplified via PCR to enhance the DNA yield. This procedure is repeated using magnetic beads linked to the HA protein of the influenza B virus, thereby creating a backup library for subsequent cycles

Table 2 Quantity of ssDNA and target protein in the SELEX process for selection of aptamers against influenza B hemagglutinin

SELEX cycle	Target protein quantity (influenza B HA protein)	Amount of ssDNA		Incubation time (min)	
	μg/mL	ng/μL	nM	Protein coupling	Library screening
1	575	29.15	1251.56	60	60
2	575	39.99	1716.4	60	60
3	288.75	34.43	1477.9	60	60
4	288.75	25.79	1106.7	50	50
5	256.67	24.37	1046	50	50
6	256.67	24.98	1072.1	45	40
7	128.33	23.86	1024.3	45	40
8	128.33	20.82	893.6	40	30

plates were then sealed with a plate-sealing membrane and incubated at 37 °C for an additional hour. After the plates were rinsed, diluted avidin-HRP solution (enzyme conjugate diluted to a ratio of 1:99) was added to each well. The plates were resealed with a plate-sealing membrane and incubated at 37 °C for another hour. Unbound avidin-HRP was removed by washing each well, after which, the substrate solution was added to seal the plate membrane. Subsequently, color was developed at 37 °C for 10–15 min. Termination solution was added based on the actual color development, ensuring that the process did not exceed 30 min. The absorbance of each well was measured using an enzyme label at a wavelength of 450 nm and the results were expressed as OD values. Data analysis was performed using GraphPad Prism 9. The binding curve was plotted according to the equation:

$Y = BmaxX/(Kd + X)$, where X represents the aptamer concentration and Y is the OD value. The Kd values were calculated from the curves.

To identify specificity, we made minor adjustments to the aforementioned protocol: the concentration of the target protein was adjusted to 25 μg/mL. Aptamer sequences were synthesized and purified. Following the manufacturer's guidelines, the aptamers were diluted in nuclease-free water and aliquots were stored at − 20 °C for further use. To determine the specificity of the selected aptamers for influenza B HA, H1N1 HA, and BSA proteins were used, and the absorbance of each well was measured at 450 nm using ELISA. All measurements were performed in triplicate, and the mean values, standard errors, and standard deviations from the mean were used to report the results.

Statistical analysis

All statistical analyses were performed using GraphPad Prism 9.1.0 for Windows (GraphPad Software, San Diego, CA, USA). Differences in OD450 across aptamers were tested using a two-tailed t-test, ANOVA, and Kruskal–Wallis test. A nonlinear curve fitting analysis of Kd was performed. The Kd value of the aptamer was determined by measuring its absorbance at 450 nm. Data are expressed as the mean ± standard deviation. Differences were considered statistically significant at $P \leq 0.05$.

Results

Selection of DNA aptamers

Starting from the second round of selection, we implemented a reverse selection strategy in each subsequent round to obtain highly specific aptamers by eliminating sequences that exhibited non-specific binding. The retention rate was determined using qPCR analysis. In this approach, the library was diluted to various concentrations, quantified using qPCR, and then employed along with their respective Cq values to construct a standard curve. The number of molecules was calculated based on the Cq values of the washed and eluted samples. The calculated number of molecules was matched with the standard curve, as shown in Fig. 2a. The retention rate is the proportion of molecules that bind to the target or anti-target during each screening iteration, relative to the total number of sequences within the input library. The results of retention validation across the nine rounds are shown in Fig. 2b. Starting from the eighth screening round, the retention rate of positive screening exceeded that of negative screening. Compared to the eighth round, the fluorescence qPCR curve in the ninth round showed an upward trend, as shown in Fig. 2c, d. High-throughput sequencing was performed on the libraries derived from the final screening phase. After sequencing, numerous alternative sequences, ranging from HA-02 to HA-48, were synthesized. Comparison of binding affinity of the blank channel with that of the target protein channel. At ambient temperature, the DNA sequences designated A012, A014, A573, A703, and A938 exhibited binding capabilities to the target protein. Five DNA sequences were identified as potential aptamers for affinity detection by SPR. As shown in Table 3.

SPR for determining affinity binding of DNA sequences

Using SPR, we observed that DNA sequences did not bind to the reference channel (treated with a blocking agent) under ambient temperature conditions. Comparative analysis of the binding of the reference channel with that of the target protein channel indicated that the A573 DNA sequence exhibited the highest affinity for the target protein at room temperature, as shown in Fig. 3a, b. Consequently, aptamer A573 was selected for further study. Additional SPR analysis of the interaction between the influenza B HA protein and A573 sequence confirmed substantial binding affinity, with a unique binding pattern visible in the gradient, as depicted in Fig. 3c.

Secondary structure of candidate aptamers

The secondary structure of the aptamer A573 was predicted using the UNAfold tool (Integrated DNA Technologies, USA). As shown in Fig. 4, the aptamer exhibited a propensity to adopt a stem-loop configuration. Stem-loop structures possess the unique ability to specifically recognize and bind to their corresponding target molecules by leveraging their distinctive spatial conformations and base-pairing arrangements. The stem-loop configuration created regions of base complementarity that contributed to the stability of the overall secondary structure of the aptamer. This stability enables the aptamer to retain a relatively constant conformation in complex biological environments, such as the presence of diverse enzymes and various ions in vivo, thus enhancing its functional capabilities. This indicated that the aptamer possessed a certain level of stability.

Aptamer A573 specificity for influenza B hemagglutinin

ELISA was used to determine the specificity of aptamer A573. Various concentrations of influenza B virus HA and H1N1 HA proteins, ranging from 100 to 6.125 μg/mL, were immobilized onto 96-well plates. Subsequent incubation with the aptamer (5′-biotin) was performed at a concentration of 20 nM. The results revealed that aptamer A573 selectively bound to the influenza B virus HA protein, and no such interaction was observed with BSA at the tested concentrations (Fig. 5a). Furthermore, aptamer A573 demonstrated a diminished binding affinity towards the H1N1 HA protein, with a statistically

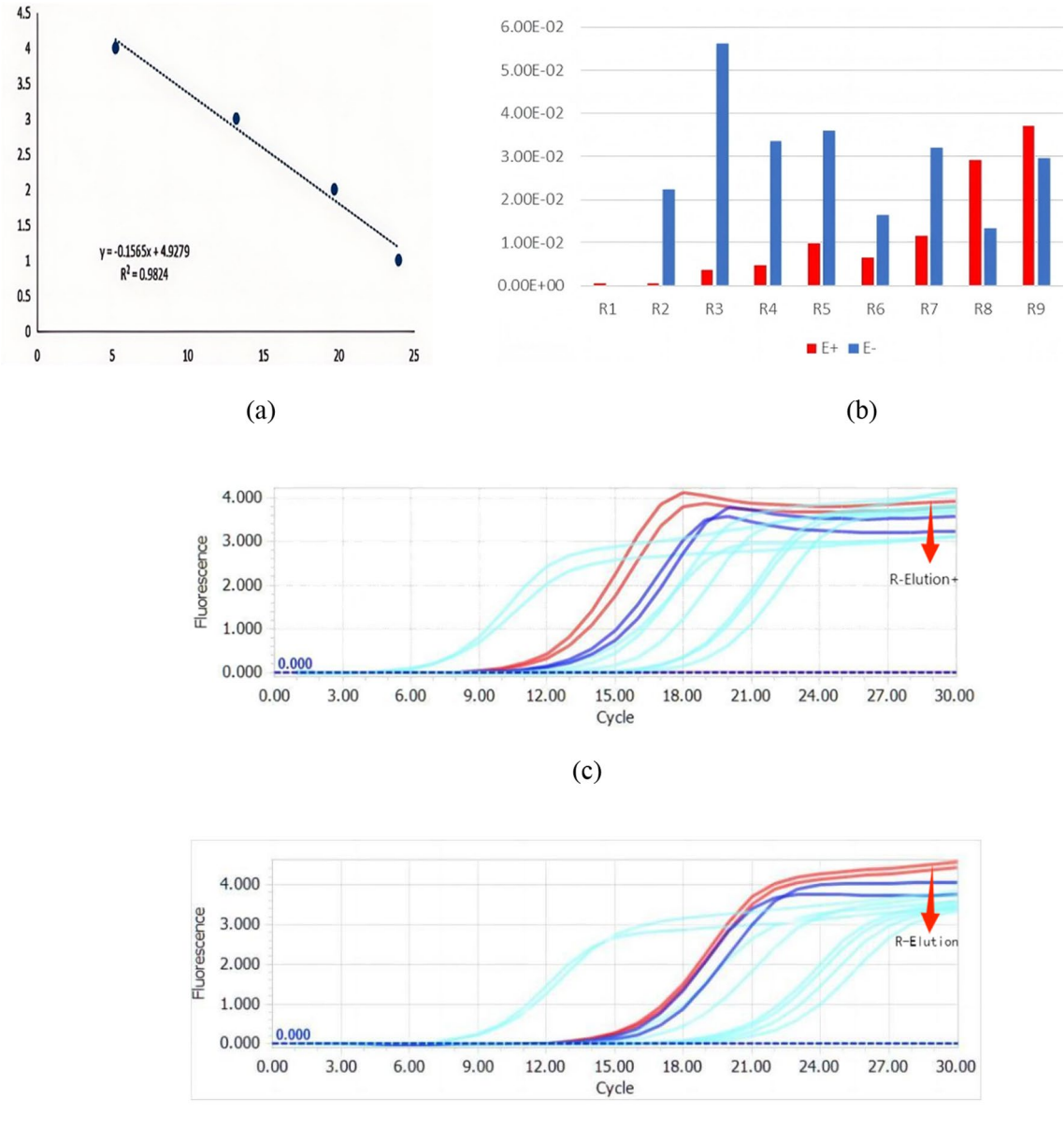

Fig. 2 Magnetic bead-SELEX screening: Retention trends and PCR curve analysis. **a** Standard curve. **b** Retention rate of the ssDNA pool following each round of SELEX. **c** Fluorescence quantitative PCR curves from the eighth round of screening. **d** Fluorescence quantitative PCR curves from the ninth round of screening

Table 3 Sequences of candidate aptamers specific for influenza B hemagglutinin

Name	Sequence (5′~3′)
A012	TTCAGCACTCCACGCATAGCCCTGACCAAGGCACGTGCTTGTCTTCCTGACAGTTACCTATGCGTGCTACCGTGAA
A014	TTCAGCACTCCACGCATAGCCCCCACCATCTGGATCTCCCGAGCTCTTCTTGACCACCTATGCGTGCTACCGTGAA
A573	TTCAGCACTCCACGCATAGCCCCCACCATCTGTATCTCCCGAGCTCTTCTTGACCACCTATGCGTGCTACCGTGAA
A703	TTCAGCACTCCACGCATAGCCATGACCAAGGCACGTGCTTGTCTTCCTGACAGTTACCTATGCGTGCTACCGTGAA
A938	TTCAGCACTCCACGCATAGCCCTGACCCAGGCACGTGCTTGTCTTCCTGACAGTTACCTATGCGTGCTACCGTGAA

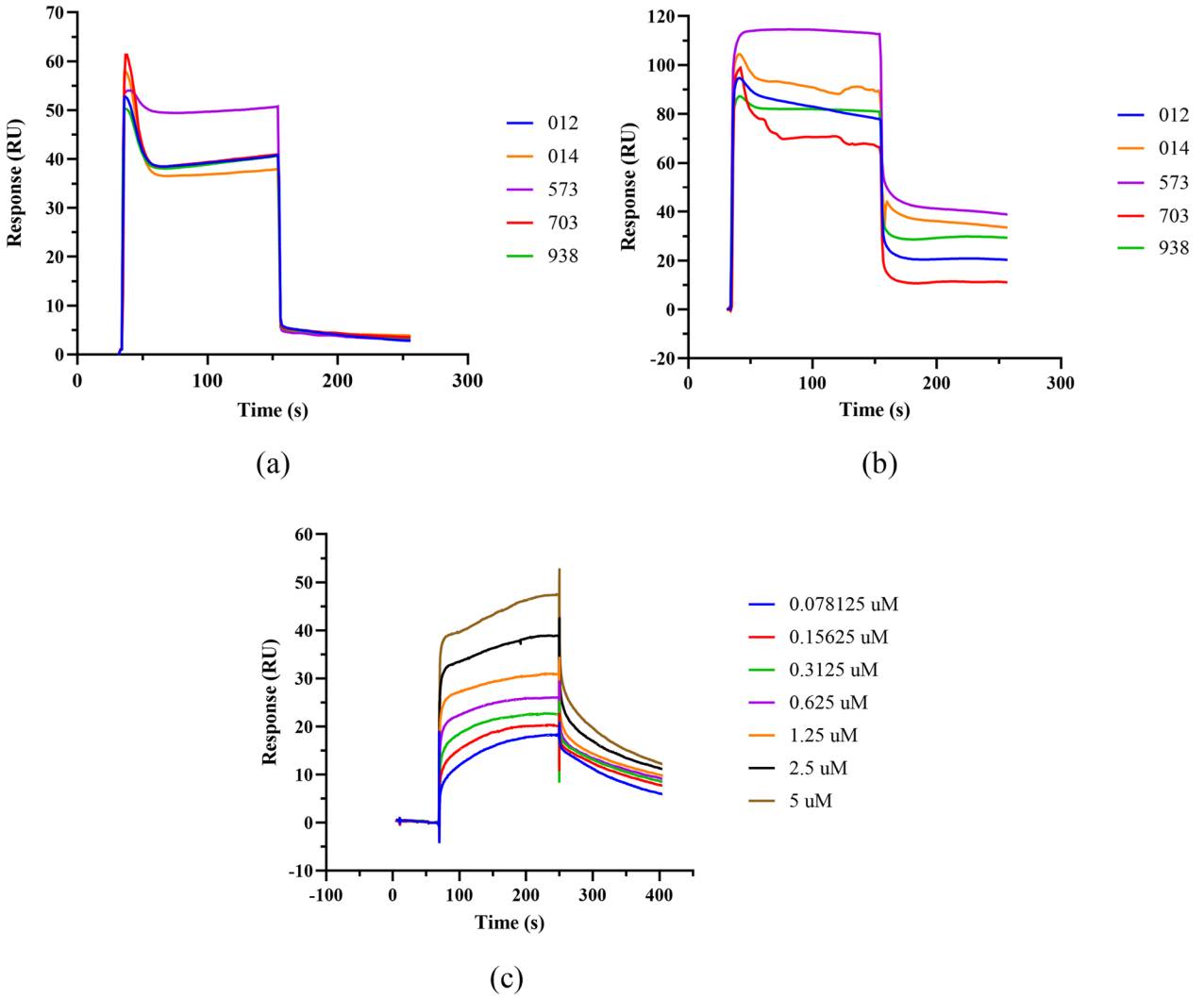

Fig. 3 SPR assay to evaluate candidate aptamer binding affinity for influenza B virus hemagglutinin protein. **a** SPR blank channel. **b** Influenza B virus HA protein channel. **c** The SPR detection of A573 exhibited a pronounced affinity for the influenza B HA protein gradient, demonstrating a distinct binding interaction

significant difference at concentrations of 25 μg/mL ($P=0.009$) and 100 μg/mL ($P=0.008$). Importantly, the binding capacity of aptamer A573 to the H1N1 HA protein was markedly lower than its affinity for the influenza B virus HA protein, particularly at 50 μg/mL ($P<0.001$). These results imply that aptamer A573 has a selective affinity for influenza B virus and does not cross-react with H1N1.

Aptamer A573 affinity for influenza B HA protein

The binding affinity of the aptamer was assessed by ELISA and quantified using the Kd value. In a 96-well microplate, influenza B virus HA proteins were immobilized at a concentration of 20 μg/mL, followed by the addition of varying concentrations of aptamer A573. OD values were recorded, and the data were analyzed using GraphPad software. Bmax signifies the maximum binding capacity and *Kd* corresponds to the concentration of the aptamer required to achieve half of the maximum binding. The *Kd* value for aptamer A573 was calculated at 10.25 nM, within the nanomolar range, with a Bmax of 0.616 (Fig. 5b).

Discussion

Influenza viruses are responsible for annual pandemics mainly due to antigenic drift. This involves the ability of the virus to evade human humoral immunity through amino acid substitutions, insertions, or deletions within

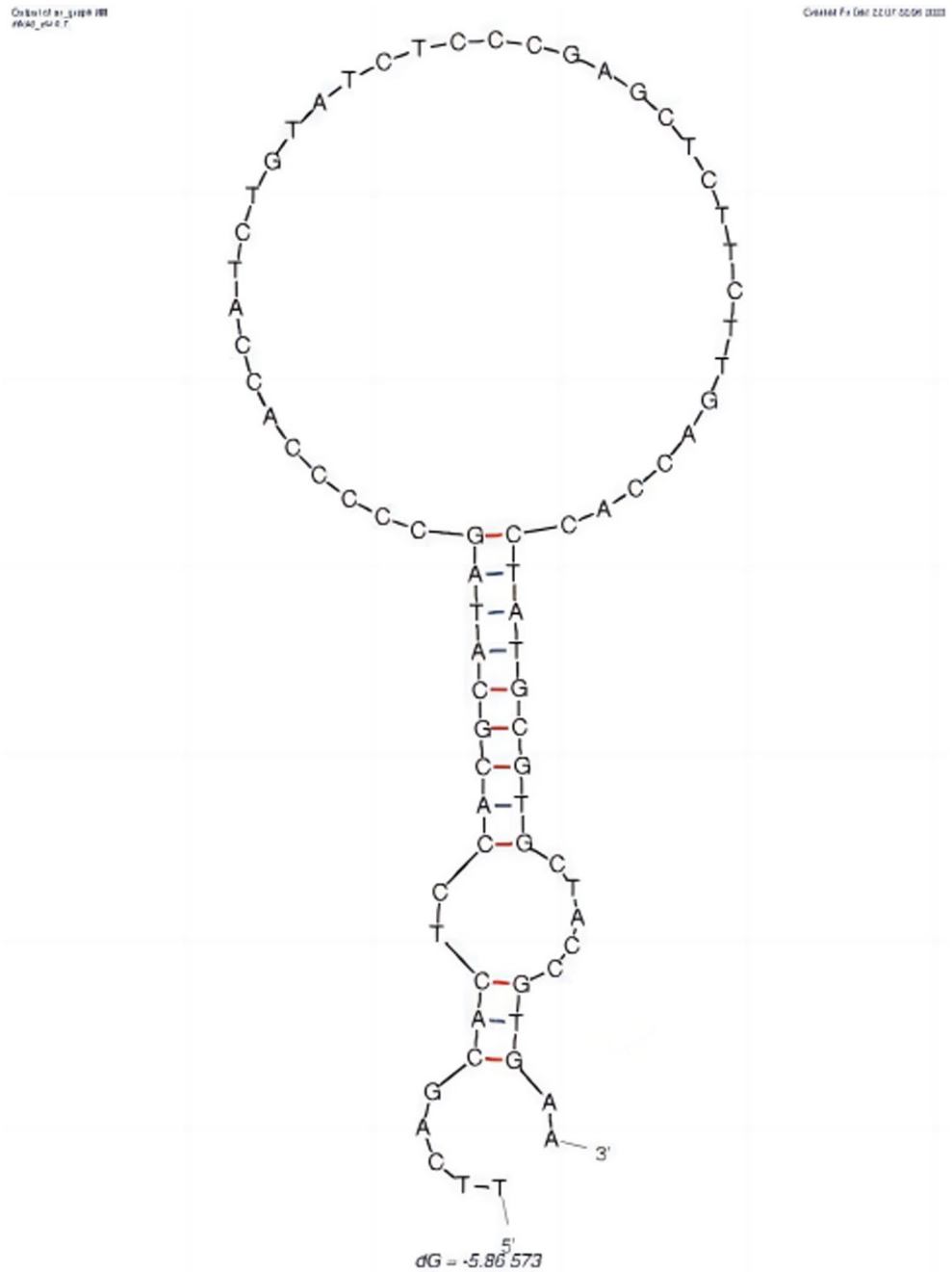

Fig. 4 Anticipated secondary structure of aptamer A573

the HA and neuraminidase epitopes. This mechanism allows the virus to bypass key antibodies generated from previous infections, vaccinations, or both [1]. The influenza B virus infects cells by binding its HA proteins to salivary acid receptors on the cell surface, followed by entry into the cell via endocytosis. Once inside the cell, viral nucleic acids are transcribed in the nucleus, leading to replication. Recent studies have identified a broad-spectrum neutralizing antibody that targets a highly conserved epitope within the HA receptor-binding site (RBS) of the influenza B viral surface antigen. This antibody showed potent antiviral activity both in vitro and in vivo [17].

In this study, we performed an in vitro SELEX screening process using a 76-nucleotide random library to identify aptamers that specifically bind to the target

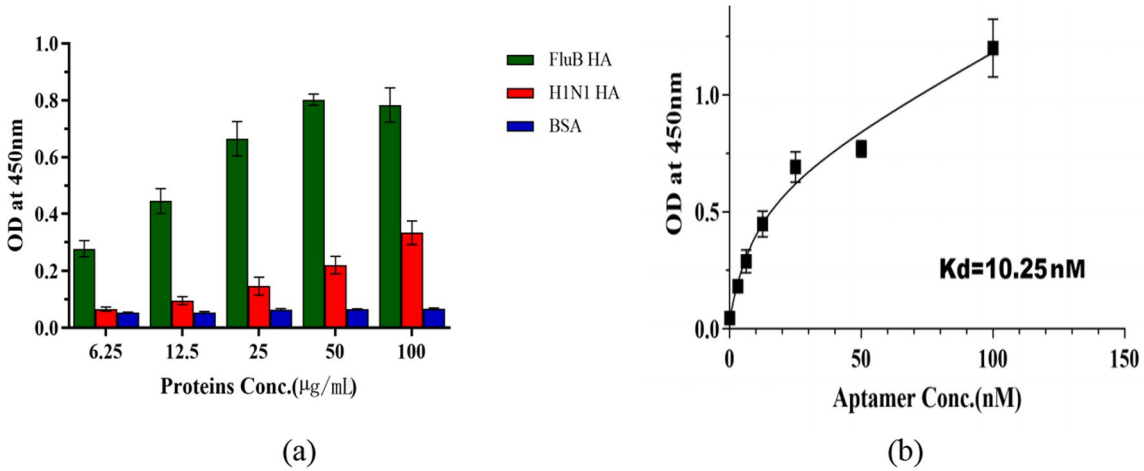

Fig. 5 Specificity assessment of aptamer A573 by ELISA. **a** The binding affinity of the aptamer A573 towards the specific influenza B virus and H1N1 HA proteins was assessed through ELISA. BSA served as a negative control (NC) in the experiments. Errors were computed based on three replicate trials. **b** ELISA was conducted to ascertain the Kd values for the influenza B virus HA protein aptamer. The data are presented as the mean ± standard deviation (SD) from three separate experiments

influenza B virus HA protein. To enhance aptamer affinity, we gradually reduced the co-incubation time between the magnetic beads and the protein, as well as between the magnetic beads and the library during screening. Furthermore, we used H1N1 HA protein as a negative control in the second phase of the screening process. The quantitative PCR amplification curve (AC) serves as a versatile monitoring instrument for various SELEX methodologies aimed at diverse targets, including small molecules, proteins, bacteria, and cancer cells [18]. Thus, qPCR ACs were used to monitor screening procedures. In the ninth SELEX cycle, we noted an increase in the qPCR curves coupled with a superior positive screening retention rate in contrast to that in the negative screening retention rate. This suggests the uniformity of the library and its unsuitability for additional screening, prompting us to cease the process and proceed with high-throughput sequencing. This led to the identification of five candidate aptamers.

The candidate aptamer A573 was selected using SPR and ELISA as the aptamer with the highest affinity and specificity for the influenza B viral HA protein. The secondary structure of A573 was predicted using bioinformatic analysis. The stem-loop structure is pivotal to the secondary structure of aptamers, as it provides highly specific recognition and binding to target molecules by leveraging their distinctive spatial conformations and base-pair arrangements. Furthermore, the stem-loop structure of an aptamer acts as a "lock" with a specific shape that corresponds to the "key" of its target molecule, which is essential for the aptamer to effectively perform its targeting function. In this study, we performed an extensive examination of various concentrations of A573, and in conjunction with the non-target molecules H1N1 HA and BSA proteins, we conducted a meticulous analysis of its specificity. The clinical manifestations and complications of seasonal influenza A and B viral infections are indistinguishable [19]. Currently, the diagnosis of influenza B virus predominantly depends on nucleic acid amplification techniques, although each of these methods has its own set of limitations. Therefore, there is an urgent need to develop novel and efficient detection methods. Aptamers are single-stranded oligonucleotides with the unique ability to specifically recognize and bind to target molecules. In the last few decades, advances in SELEX technology have included the modification of oligonucleotide strand libraries, broadening of the target spectrum, reduction in screening duration, and enhancement of aptamer stability. These technological improvements have significantly enhanced the screening efficiency, paving the way for limitless opportunities in the acquisition of aptamers. Aptamers offer several advantages, including their flexible structure, ease of chemical synthesis and modification, excellent stability, and non-immunogenic properties [20–24]. They have found widespread applications in various biomedical fields, including analytical detection [25, 26], disease diagnosis [27], treatment [28–30], and inhibition of influenza viruses [31–33]. In this study, aptamers exhibiting high affinity and specificity for influenza B viral HA were identified and thoroughly characterized. These aptamers hold promise as key recognition elements for the development of rapid detection systems such as aptamer-based sensors.

Conclusions

In the present study, we used the SELEX technique to identify aptamer sequences that specifically target the influenza B viral HA protein. Initially, we employed SPR technology to assess the affinity of alternative DNA sequences obtained during screening. We identified aptamer A573 with the highest binding affinity for the target protein. We further conducted a secondary structure prediction analysis of aptamer A573. Finally, through ELISA, we observed that aptamer A573 demonstrated the highest sensitivity in binding to the target protein with the highest affinity. In the present study, only the pertinent aptamers underwent in vitro testing; subsequent validation of the functionality of the selected aptamers necessitates their combination with human specimens. The aptamers identified in this study have potential value for use in sensors for the early detection and treatment of influenza B. Under favorable conditions, we intend to incorporate nucleic acid aptamers into sensor technology, with the objective of developing a device capable of rapid detection of influenza B virus.

Abbreviations

AC	Amplification curve
APS	Ammonium persulfate
BSA	Bovine serum albumin
DPBS	Dulbecco's phosphate-buffered saline
ELISA	Enzyme-linked immunosorbent assay
HA	Hemagglutinin
OD	Optical density
RBS	Receptor-binding site
RNA	Ribonucleic acid
SELEX	Systematic evolution of ligands by exponential enrichment
SPR	Surface plasmon resonance
ssDNA	Single-stranded deoxyribonucleic acid
TEMED	*N,N,N′,N′*-tetramethylethylenediamine

Acknowledgements

Not applicable.

Author contributions

XL: Conceptualization, Formal analysis, Investigation, Visualization, Writing—Original draft, Writing—Reviewing & editing; WL: Formal analysis, Investigation, Writing—Reviewing & editing; PL: Investigation, Writing—Reviewing & editing; YL: Investigation, Visualization, YG: Methodology, Investigation; TW: Resources, Investigation; ZL: Supervision, Resources, Project administration; YW: Writing—Reviewing & editing, Supervision, Funding acquisition, Conceptualization.

Funding

Not applicable.

Availability of data and materials

No datasets were generated or analysed during the current study.

Declarations

Ethics approval and consent to participate

Not applicable.

Consent for publication

Not applicable.

Competing interests

The authors declare no competing interests.

Received: 3 June 2024 Accepted: 10 February 2025
Published online: 07 March 2025

References

1. Uyeki TM, Hui DS, Zambon M, Wentworth DE, Monto AS. Influenza. Lancet. 2022;400:693–706. https://doi.org/10.1016/S0140-6736(22)00982-5.
2. Hensen L, Kedzierska K, Koutsakos M. Innate and adaptive immunity toward influenza B viruses. Future Microbiol. 2020;15:1045–58. https://doi.org/10.2217/fmb-2019-0340.
3. Wang X, Yin X, Zhang BY, et al. A prophylactic effect of aluminium-based adjuvants against respiratory viruses via priming local innate immunity. Emerg Microbes Infect. 2022;11:914–25.
4. Kosik I, Yewdell JW. Influenza hemagglutinin and neuraminidase: Yin–Yang proteins coevolving to thwart immunity. Viruses. 2019;11:346. https://doi.org/10.3390/v11040346.
5. Paules C, Subbarao K. Influenza. Lancet. 2017;390:697–708. https://doi.org/10.1016/S0140-6736(17)30129-0.
6. Zaraket H, Hurt AC, Clinch B, Barr I, Lee N. Burden of influenza B virus infection and considerations for clinical management. Antiviral Res. 2021;185:104970. https://doi.org/10.1016/j.antiviral.2020.104970.
7. Caini S, Kusznierz G, Garate VV, Wangchuk S, Thapa B, de Paula Júnior FJ, et al. The epidemiological signature of influenza B virus and its B/Victoria and B/Yamagata lineages in the 21st century. PLoS ONE. 2019;14:e0222381. https://doi.org/10.1371/journal.pone.0222381.
8. Pormohammad A, Ghorbani S, Khatami A, Razizadeh MH, Alborzi E, Zarei M, et al. Comparison of influenza type A and B with COVID-19: a global systematic review and meta-analysis on clinical, laboratory and radiographic findings. Rev Med Virol. 2021;31:e2179. https://doi.org/10.1002/rmv.2179.
9. Liu X, Hou Y, Chen S, Liu J. Controlling dopamine binding by the new aptamer for a FRET-based biosensor. Biosens Bioelectron. 2021;173:112798. https://doi.org/10.1016/j.bios.2020.112798.
10. Huang Y, Zheng J, Wang L, Duan X, Wang Y, Xiang Y, et al. Sensitive detection of chloramphenicol based on Ag-DNAzyme-mediated signal amplification modulated by DNA/metal ion interaction. Biosens Bioelectron. 2019;127:45–9. https://doi.org/10.1016/j.bios.2018.12.016.
11. Zhou J, Rossi J. Aptamers as targeted therapeutics: current potential and challenges. Nat Rev Drug Discov. 2017;16:181–202. https://doi.org/10.1038/nrd.2016.199 [published correction appears in Nat Rev Drug Discov. 2017;16:440. https://doi.org/10.1038/nrd.2017.86]
12. Zhuo Z, Yu Y, Wang M, Li J, Zhang Z, Liu J, et al. Recent advances in SELEX technology and aptamer applications in biomedicine. Int J Mol Sci. 2017;18:2142. https://doi.org/10.3390/ijms18102142.
13. Yan J, Xiong H, Cai S, Wen N, He Q, Liu Y, et al. Advances in aptamer screening technologies. Talanta. 2019;200:124–44. https://doi.org/10.1016/j.talanta.2019.03.015.
14. Zou X, Wu J, Gu J, Shen L, Mao L. Application of aptamers in virus detection and antiviral therapy. Front Microbiol. 2019;10:1462. https://doi.org/10.3389/fmicb.2019.01462.
15. Shi L, Wang L, Ma X, Fang X, Xiang L, Yi Y, et al. Aptamer-functionalized nanochannels for one-step detection of SARS-CoV-2 in samples from COVID-19 patients. Anal Chem. 2021;93:16646–54. https://doi.org/10.1021/acs.analchem.1c04156.
16. Bhardwaj J, Chaudhary N, Kim H, Jang J. Subtyping of influenza A H1N1 virus using a label-free electrochemical biosensor based on the DNA aptamer targeting the stem region of HA protein. Anal Chim Acta. 2019;1064:94–103. https://doi.org/10.1016/j.aca.2019.03.005.
17. Shen C, Chen J, Li R, Zhang M, Wang G, Stegalkina S, et al. A multimechanistic antibody targeting the receptor binding site potently cross-protects against influenza B viruses. Sci Transl Med. 2017;9:eaam5752. https://doi.org/10.1126/scitranslmed.aam5752.
18. Luo Z, He L, Wang J, Fang X, Zhang L. Developing a combined strategy for monitoring the progress of aptamer selection. Analyst. 2017;142:3136–9. https://doi.org/10.1039/c7an01131h.

19. Su S, Chaves SS, Perez A, D'Mello T, Kirley PD, Yousey-Hindes K, et al. Comparing clinical characteristics between hospitalized adults with laboratory-confirmed influenza A and B virus infection. Clin Infect Dis. 2014;59:252–5. https://doi.org/10.1093/cid/ciu269.
20. Wang T, Chen C, Larcher LM, Barrero RA, Veedu RN. Three decades of nucleic acid aptamer technologies: lessons learned, progress and opportunities on aptamer development. Biotechnol Adv. 2019;37:28–50. https://doi.org/10.1016/j.biotechadv.2018.11.001.
21. Morita Y, Leslie M, Kameyama H, Volk DE, Tanaka T. Aptamer therapeutics in cancer: current and future. Cancers (Basel). 2018;10:80. https://doi.org/10.3390/cancers10030080.
22. Röthlisberger P, Hollenstein M. Aptamer chemistry. Adv Drug Deliv Rev. 2018;134:3–21. https://doi.org/10.1016/j.addr.2018.04.007.
23. Liu M, Yu X, Chen Z, Yang T, Yang D, Liu Q, et al. Aptamer selection and applications for breast cancer diagnostics and therapy. J Nanobiotechnology. 2017;15:81. https://doi.org/10.1186/s12951-017-0311-4.
24. Acquah C, Agyei D, Obeng EM, Pan S, Tan KX, Danquah MK. Aptamers: an emerging class of bioaffinity ligands in bioactive peptide applications. Crit Rev Food Sci Nutr. 2020;60:1195–206. https://doi.org/10.1080/10408398.2018.1564234.
25. Mairal T, Ozalp VC, Lozano Sánchez P, Mir M, Katakis I, O'Sullivan CK. Aptamers: molecular tools for analytical applications. Anal Bioanal Chem. 2008;390:989–1007. https://doi.org/10.1007/s00216-007-1346-4.
26. Huang PJJ, Liu J. Simultaneous detection of L-lactate and D-glucose using DNA aptamers in human blood serum. Angew Chem Int Ed Engl. 2023;62:e202212879. https://doi.org/10.1002/anie.202212879.
27. Peinetti AS, Lake RJ, Cong W, Cooper L, Wu Y, Ma Y, et al. Direct detection of human adenovirus or SARS-CoV-2 with ability to inform infectivity using DNA aptamer-nanopore sensors. Sci Adv. 2021;7:eabh2848. https://doi.org/10.1126/sciadv.abh2848.
28. Sun H, Zhu X, Lu PY, Rosato RR, Tan W, Zu Y. Oligonucleotide aptamers: new tools for targeted cancer therapy. Mol Ther Nucleic Acids. 2014;3:e182. https://doi.org/10.1038/mtna.2014.32.
29. Bohrmann L, Burghardt T, Haynes C, Saatchi K, Häfeli UO. Aptamers used for molecular imaging and theranostics—recent developments. Theranostics. 2022;12:4010–50. https://doi.org/10.7150/thno.72949.
30. Asha K, Kumar P, Sanicas M, Meseko CA, Khanna M, Kumar B. Advancements in nucleic acid based therapeutics against respiratory viral infections. J Clin Med. 2018;8:6. https://doi.org/10.3390/jcm8010006.
31. Pan Q, Luo F, Liu M, Zhang XL. Oligonucleotide aptamers: promising and powerful diagnostic and therapeutic tools for infectious diseases. J Infect. 2018;77:83–98. https://doi.org/10.1016/j.jinf.2018.04.007.
32. Chakraborty B, Das S, Gupta A, Xiong Y, T-v V, Kizer ME, et al. Aptamers for viral detection and inhibition. ACS Infect Dis. 2022;8:667–92. https://doi.org/10.1021/acsinfecdis.1c00546.
33. Li W, Feng X, Yan X, Liu K, Deng L. A DNA aptamer against influenza A virus: an effective inhibitor to the hemagglutinin-glycan interactions. Nucleic Acid Ther. 2016;26:166–72. https://doi.org/10.1089/nat.2015.0564.

Publisher's Note